Vascular Pharmacology 128–129 (2020) 106675

Contents lists available at ScienceDirect

Vascular Pharmacology

journal homepage: www.elsevier.com/locate/vph

Maslinic acid suppresses macrophage foam cells formation: Regulation of monocyte recruitment and macrophage lipids homeostasis

Su Wen Phang[a], Bee Kee Ooi[a], Nafees Ahemad[b], Wei Hsum Yap[a,*]

[a] School of Biosciences, Taylor's University, Subang Jaya, Selangor Darul Ehsan 47500, Malaysia
[b] School of Pharmacy, Monash University Malaysia, Bandar Sunway, Selangor Darul Ehsan 47500, Malaysia

ARTICLE INFO

Keywords:
Foam cells
Maslinic acid (MA)
Monocyte recruitment
Antioxidant
LDL oxidation
Cholesterol efflux

ABSTRACT

The transformation of macrophages to foam cells is a critical component in atherosclerotic lesion formation. Maslinic acid (MA), a novel natural pentacyclic triterpene, has cardioprotective and anti-inflammatory properties. It is hypothesized that MA can suppress monocyte recruitment to endothelial cells and inhibit macrophage foam cells formation. Previous study shows that MA inhibits inflammatory effects induced by sPLA2-IIA, including foam cells formation. This study elucidates the regulatory effect of MA in monocyte recruitment, macrophage lipid accumulation and cholesterol efflux. Our findings demonstrate that MA inhibits THP-1 monocyte adhesion to HUVEC cells in a TNFα-dependent and independent manner, but it induces trans-endothelial migration marginally at low concentration. MA down-regulates both gene and protein expression on VCAM-1 and MCP-1 in HUVECs. We further showed that MA suppresses macrophage foam cells formation, as indicated from the Oil-Red-O staining and flow cytometric analysis of intracellular lipids accumulation. The effects observed may be attributed to the antioxidant properties of MA where it was shown to suppress $CuSO_4$-induced lipid peroxidation. MA inhibits scavenger receptors SR-A and CD36 expression while enhancing cholesterol efflux. MA enhances cholesterol efflux transporters ABCA1 and ABCG1 genes expression marginally without inducing its protein expression. In this study, MA was shown to target important steps that contribute to foam cell formation, including its ability in reducing monocytes adhesion to endothelial cells and LDL peroxidation, down-regulating scavenger receptors expression as well as enhancing cholesterol efflux, which might be of great importance in the context of atherosclerosis prevention and treatment.

1. Introduction

Atherosclerosis is characterized by the thickening of arterial wall caused by accumulation of cholesterol which leads to plaque formation. It is a major risk factor that contributes to cardiovascular diseases including peripheral arterial disease, ischemic heart disease, stroke and heart attack [1]. According to the World Health Organization 2016, there are an estimated of 17.9 million people deaths due to cardiovascular diseases, accounting for 31% of all global deaths and out of these deaths, 85% are mainly due to heart attack and stroke. It is postulated that inflammatory monocytes are the major cellular component in the atherosclerotic plaques.

At the inflammatory atherosclerotic lesion sites, pro-inflammatory cytokines such as interleukin (IL)-1, interferon (IFN), tumor necrosis factor (TNF) and chemokines are essential in mediating cell-cell interactions such as monocyte recruitment, adhesion and migration. Multiple immune cell types including monocytes, macrophages, dendritic cells, and lymphocytes that are involved in atherosclerotic lesion development produce and respond to these cytokines; excessive amount of cytokines can be found in these lesion sites [2,3]. For instance, IL-1 and TNF-α released by monocytes or macrophages induce expression of pro-inflammatory genes TNF-α, COX-2, inducible forms of nitric oxide synthase (iNOS), and IL-6 which are involved in cell injury, infections, immune-activated T cells and ischemic heart diseases [4,5].

Inflammatory stimuli including lipopolysaccharide, TNF-α, and IL-1β would induce endothelial activation and subsequently up-regulate the expression of adhesion molecules and chemokines, including P-selectin, E-selectin, vascular cell adhesion molecule-1 (VCAM-1), and intercellular adhesion molecule-1 (ICAM-1), leading to monocyte recruitment and transmigration to the sub-endothelial layer [6–8]. Endothelium activation also facilitates modification and oxidation of LDL accumulated within the sub-endothelial layer and resulting in progressive accumulation of lipids-loaded macrophages, leading to the formation of fatty streaks [8]. As inflammation progresses, vascular

* Corresponding author.
E-mail addresses: nafees.ahemad@monash.edu (N. Ahemad), weihsum.yap@taylors.edu.my (W.H. Yap).

https://doi.org/10.1016/j.vph.2020.106675
Received 30 October 2019; Received in revised form 20 February 2020; Accepted 17 March 2020
Available online 19 March 2020

smooth muscle cells migrate into the intima and produce extracellular matrix that forms the fibrous layer covering the fatty streaks, and subsequently develops into atherosclerotic plaque [9].

MA is a natural pentacyclic triterpene found in various natural sources, ranging from herbal remedies to edible vegetables and fruits [10]. It has been systematically studied for its beneficial effects, including antioxidant, antitumoral, anti-inflammatory, cardioprotective, and antiviral properties [10–15]. MA has potential anti-inflammatory and antioxidant properties that protects against cardiovascular diseases as reported in several in vivo and in vitro studies. The protective effect of MA against isoproterenol (ISO)-induced cardiotoxicity and the association between paraoxonase (PON) status and MA supplementation was first reported by Hussain Shaik et al. [16]. Pre-treatment with MA decreased the levels of total cholesterol, triglycerides, LDL-C, and VLDL-C and increased the levels of HDL-C in ISO-administered rats. These cardioprotective changes may be due to the anti-hyperlipidemic effects of MA [17]. MA has also been shown to suppress the expression of TNF-α, reduce phosphorylation of IκBα and inhibit p65 translocation to the nucleus in primary cortical astrocytes. In addition, MA inhibits LPS-induced formation of NO, as well as mRNA and protein levels of inducible nitric oxide (iNOS) and COX-2 [13].

It is hypothesized that MA is able to target macrophage foam cell formation process through suppressing TNF-α-mediated monocyte recruitment and transmigration to endothelial cells, LDL oxidation while enhancing cholesterol efflux from lipid-loaded macrophages. The aim of this study was to investigate the mechanism of MA in TNF-α-mediated adhesion and migration of monocytes to endothelial cells as well as its effect on macrophage foam cells formation.

2. Materials and methods

2.1. Cell culture

Human umbilical vein endothelial cells (HUVECs) and human monocytic cell line THP-1 were purchased from the American Type Culture Collection (ATCC). HUVECs were maintained in Endothelial Cell Growth Medium Bullet Kit supplemented with Bovine Brain Extract (BBE), Ascorbic Acid, Hydrocortisone, human Epidermal Growth Factor (hEGF), Fetal Bovine Serum (FBS) and Gentamicin/Amphotericin-B (GA) (Lonza, USA). THP-1 monocytes and PMA-differentiated THP-1 macrophages were maintained in RPMI-1640 medium supplemented with 2.0 g/L sodium bicarbonate (Sigma, US) and 10% FBS (Sigma-Aldrich, Europe). THP-1 cells (3.0×10^5 cells/mL) were differentiated into macrophages in 24-well culture plate containing 100 ng/mL of PMA in 1 mL RPMI-1640 medium for 72 h. All cells were cultured in 5% CO_2 incubator under 37 °C.

2.2. Resazurin cell viability assay

HUVECs, THP-1 monocytes and PMA-differentiated THP-1 macrophages were treated with various concentrations of MA (1 μM, 10 μM, 20 μM, 50 μM; Cayman Chemical, Michigan, USA). HUVECs (1.0×10^4 cells/well) and THP-1 cells (1.0×10^5 cells/well) were seeded in 96-well culture plates and treated with MA for 24 h at 37 °C in a humidified 5% CO_2 incubator. PMA-differentiated THP-1 macrophages (3.0×10^5 cells/well) were seeded in 24-well culture plates and treated with MA for 24 h at 37 °C in a humidified 5% CO_2 incubator. Cell viability was determined after 24 h incubation by adding 20 μL (96-well culture plate) and 100 μL (24-well culture plate) of resazurin respectively (0.15 mg/mL, final concentration; Sigma-Aldrich, US) into each well and further incubated for 3 h in dark. The percentage cell viability was determined by measuring the fluorescence intensity at 550 nm excitation/599 nm emission wavelength using BMG FLUOstar OPTIMA Microplate Reader. Percentage cell viability was calculated by normalizing the fluorescence values to non-treated cell samples (100% cell viability).

2.3. Monocyte adhesion and trans-endothelial migration

2.3.1. Monocyte adhesion assay

HUVECs (1.0×10^4 cells/well) were seeded in a 96-well culture plate and grown to confluence prior to experimental treatments. Meanwhile, THP-1 cells (1.0×10^5 cells/well) were labeled with 1 μM Calcein-AM (Corning, US) and incubated for 30 min at 37 °C, 5% CO_2. Labeled THP-1 cells will then be co-incubated with the confluent HUVEC monolayer pre-treated with 20 ng/mL TNF-α and various concentrations of MA (5 and 10 μM) for 1 h at 37 °C. The 96-well plate is then gently washed with PBS solution twice to remove the non-adherent THP-1 cells. The fluorescence of adhered THP-1 cells per well will be measured at 492 nm excitation/535 nm emission using BMG FLUOstar OPTIMA plate reader. The percentage of monocytes adhesion was calculated by normalizing the fluorescence values to non-treated control group.

2.3.2. Trans-endothelial migration assay

HUVECs (1.0×10^4 cells/insert) were seeded into the upper chamber of 24-well transwell culture plate (BD BioCoat™, 8.0 μm pore size) coated with a combination of 20 ng/mL fibronectin and 0.1% (*w/v*) gelatin in endothelial growth medium. Culture media was changed every two days until they have become a confluent monolayer. The HUVEC monolayer were then loaded with Calcein-labeled THP-1 cells (1.0×10^5 cells/insert) and transferred to fresh transwell containing RPMI medium. Both HUVEC and labeled THP-1 cells were co-incubated in the presence or absence of TNF-α and 20 μM of MA and incubated at 37 °C in a humidified incubator with 5% CO_2 for 3 h and migration of THP-1 through the endothelium was determined by quantifying fluorescence at 492 nm excitation/535 nm emission (bottom reading mode) using Fluostar OPTIMA plate reader.

2.4. LDL isolation

Native-LDL (nLDL) was isolated from the plasma by gradient density ultracentrifugation. Briefly, fasting peripheral venous blood samples were collected from healthy volunteers prior for ultracentrifugation. The red blood cells and plasma were separated by centrifugation at 2700 rpm for 15 min at room temperature. The plasma was transferred into a new tube, and followed by a second centrifugation step at 3300 rpm for 10 min to remove any residual intact blood cells which were carried over from the first centrifugation. The plasma was used immediately for ultracentrifugation or frozen overnight at −80 °C before use. The plasma density was then adjusted to 1.35 g/mL with solid KBr. A total of 3.5 mL plasma was transferred into a 13.2 mL polyallomer ultracentrifuge tube (Beckman Coulter, USA). A discontinuous gradient was formed by carefully layering 2 mL of 1.22 g/mL KBr solution, 4 mL of 1.063 g/mL KBr solution and 2 mL of 1.006 g/mL KBr solution. Ultracentrifugation was then performed in a SW40 Ti swinging-bucket rotor (Beckman Coulter, USA) at 40,000 rpm for 6 h at 4 °C. After ultracentrifugation, the tubes were carefully removed from rotor and the fractions were collected. The densities of collected fractions were then measured. The collected fractions were dialyzed by Pur-A-Lyzer maxi dialysis kit (Sigma-Aldrich, USA) in dark for 24 h at 4 °C against three changes of 750 mL 0.01 M PBS. All fractions were filtered by 0.2 μm Millipore CA membrane. The LDL fractions were either used immediately or stored at −80 °C. The protein concentration of nLDL was determined by using Pierce BCA Protein Assay Kit (Thermo Scientific, USA).

2.5. LDL oxidation and TBARS measurement

Copper (II) sulphate ($CuSO_4$)-induced low density liproprotein (LDL) oxidation was performed by diluting nLDL with phosphate buffer saline (PBS) to a concentration of 2.0 mg/mL before oxidation. Native LDL was incubated with $CuSO_4$ (50 μM, final concentration; Sigma-

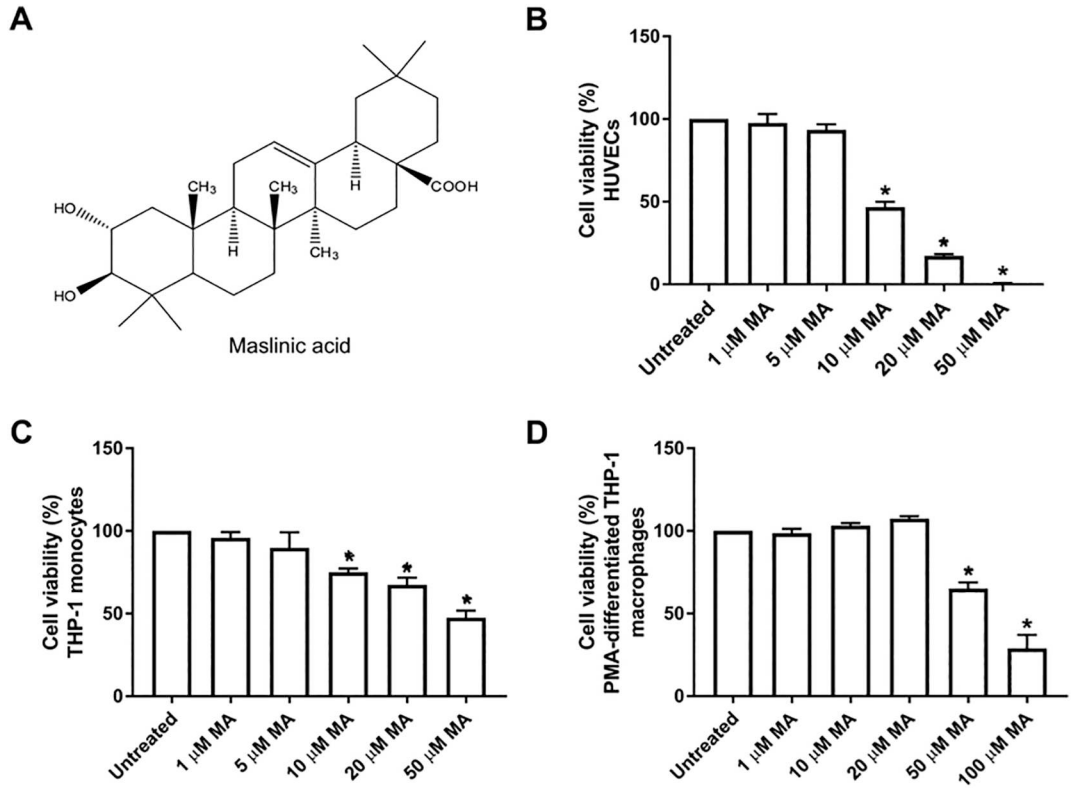

Fig. 1. Cytotoxic effects of MA on HUVECs, THP-1 monocytes and PMA-differentiated THP-1 macrophages. (**A**) Structure of MA. (**B**) HUVECs, (**C**) THP-1 monocytes and (**D**) PMA-differentiated THP-1 macrophages were treated with different concentrations of MA (1 μM, 5 μM, 10 μM, 20 μM, 50 μM, 100 μM) for 24 h at 37 °C in a humidified 5% CO_2 incubator. The percentage cell viability was determined by Resazurin assay. The cell viability was analyzed by measuring the fluorescence intensity at 550 nm excitation/599 nm emission wavelength using BMG FLUOstar OPTIMA Microplate Reader. Values represent means ± SD of three independent experiments performed in triplicates. Statistical significance was determined using One-way ANOVA followed by a Tukey's test. * represents $p < .05$ compared to untreated cells.

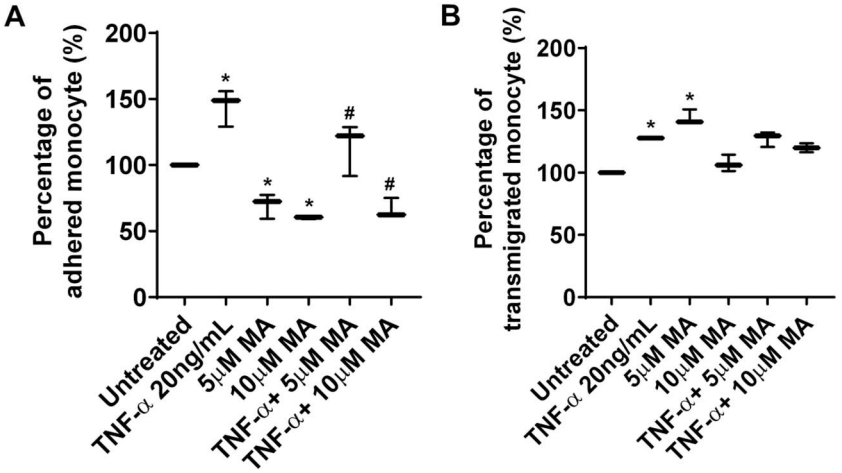

Fig. 2. MA inhibits TNF-α-induced monocyte adhesion to endothelial cells without affecting trans-endothelial migration. (**A**) HUVECs were treated with 20 ng/mL recombinant human TNF-α and various concentrations of MA (5 and 10 μM) for 24 h and then co-incubated with Calcein-labeled THP-1 monocytes for additional 1 h to allow adhesion of THP-1 monocytes to HUVECs. (**B**) HUVECs were treated with 20 ng/mL recombinant human TNF-α and various concentrations of MA (5 and 10 μM) for 24 h on 8.0 μm pore size Transwell inserts (BD BioCoat™) and then co-incubated with Calcein-labeled THP-1 monocytes for additional 3 h to allow migration of THP-1 monocytes through HUVECs. The fluorescence of adhered and migrated Calcein-labeled THP-1 monocytes was measured at 492 nm excitation/535 nm emission using BMG FLUOstar OPTIMA Microplate Reader. Values represent means ± SD of three independent experiments performed in triplicates. Statistical significance was determined by One-way ANOVA followed by a Tukey's test where several experimental groups were compared to the control group. * represents $p < .05$ compared to untreated cells. # represents $p < .05$ compared to TNF-α-induced HUVECs.

Aldrich, US) and various concentrations of MA (1, 10 and 20 μM) together at 37 °C for 24 h in dark. The extent of LDL oxidation was determined by measuring malondialdehyde (MDA) (Cayman Chemical, Michigan, USA), the end product of lipid peroxidation using thiobarbituric acid-reactive substances (TBARS) assay. The TBARS assay was carried out by mixing 50 μL of blank, MDA standards and LDL samples with 250 μL of 0.78% (*w/v*) TBA (Merck, Germany) and 250 μL of 20% (*v/v*) acetic acid. Fresh solution of TBA was prepared for each test. The blank, standards and samples were heated at 95 °C for 45 min and centrifuged at 4000 rpm for 5 min. 150 μL supernatant fractions were transferred to a 96-well culture plate and the absorbance was measured using Epoch" 2 microplate spectrophotometer at wavelength of 532 nm. The amount of the end product of lipid peroxidation was determined from MDA standard curve and the results were calculated as nmol MDA/ mg LDL protein.

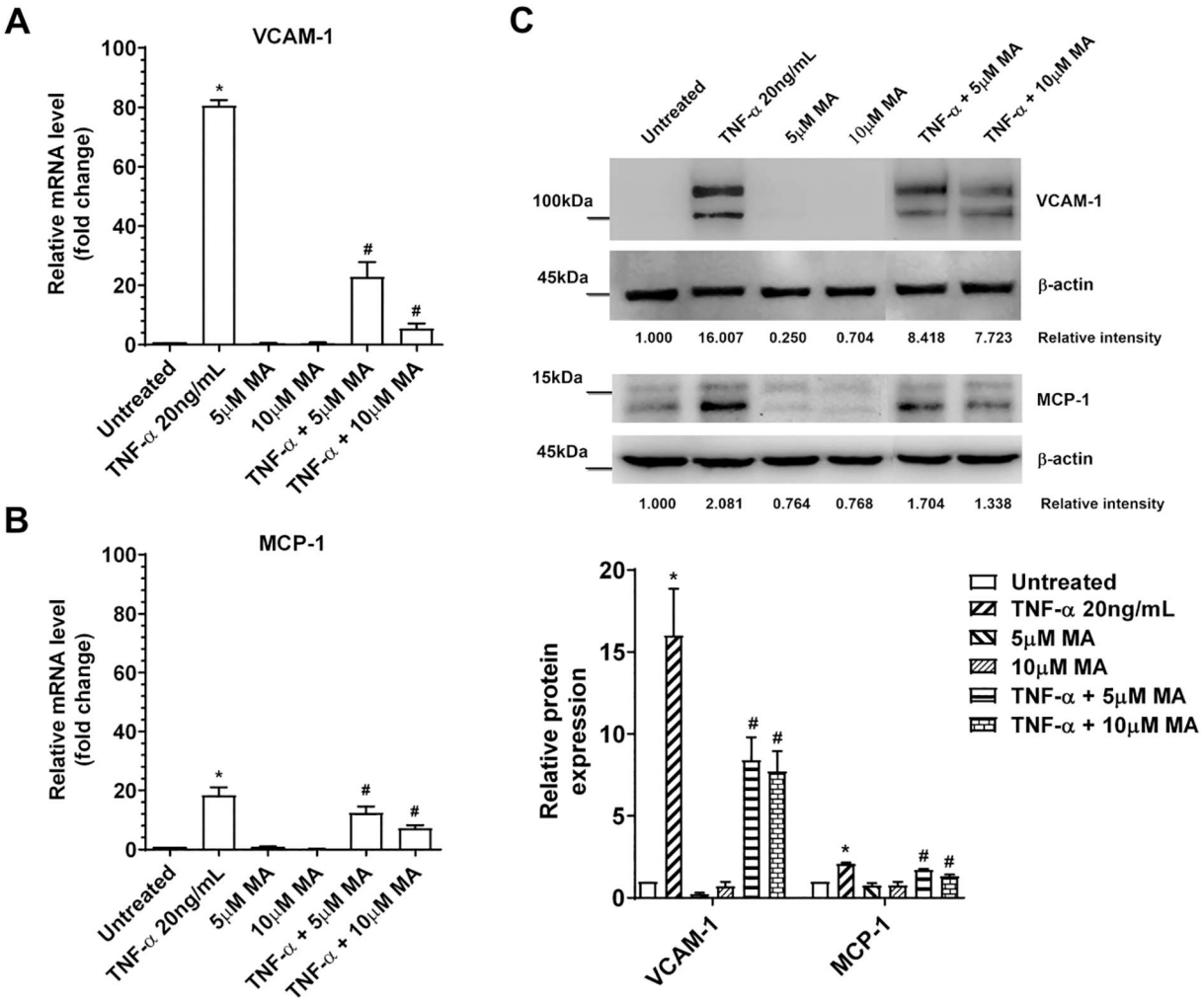

Fig. 3. MA downregulates adhesion and migration factors. (**A**) and (**B**) represent RT-qPCR analysis of VCAM-1 and MCP-1 genes expression in HUVECs with different treatments. (**C**) represents Western blot analysis of VCAM-1 and MCP-1 proteins expression in HUVECs with different treatments. Relative intensity, represented by the band intensity in Western blot, is summarized in the box plot. β-actin (45 kDa) served as the loading control. Values represent means ± SD of three independent experiments performed in triplicates. Statistical significance was determined by One-way ANOVA followed by a Tukey's test where several experimental groups were compared to the control group. * represents $p < .05$ compared to untreated cells. # represents $p < .05$ compared to TNF-α-induced HUVECs.

2.6. Optimized foam cells assay by Oil-red-O staining

THP-1 monocytes (3×10^5 cells/well) were seeded in 24-well culture plate and differentiated into macrophages with 100 ng/mL phorbol 12-myristate 13-acetate (PMA) for 72 h. PMA-differentiated THP-1 macrophages were further incubated with nLDL and oxLDL in the presence or absence of 20 μM MA for 24 h. ORO staining was performed to determine intracellular lipids accumulation in PMA-differentiated THP-1 macrophages. Briefly, ORO stock solution was prepared by dissolving 0.5 g ORO powder (Sigma, USA) in 80 mL of 100% isopropanol in water bath at a temperature of 56 °C overnight. The final volume of the stock was adjusted to 100 mL. A working solution was prepared by diluting the stock solution with the ration of three parts of ORO stock and two parts of deionized water and allowed to sit at room temperature for 10 min and then filtered. The working solution was prepared fresh and used within 2 h of preparation. The PMA-differentiated THP-1 macrophages were washed with PBS and fixed with 10% (*v*/v) paraformaldehyde for 30 min. The cells were rinsed in PBS twice and then incubated with 60% isopropanol for 15 s. The isopropanol were removed and cells were exposed to ORO working solution for 30 min in dark. ORO-stained cells were distained with 60% (v/v) isopropanol for 15 s and rinsed with deionized water several times to wash off excess stain. Macrophage-derived foam cells were stained red (positive staining) under Eclipse-Ti inverted microscope. Images of PMA-differentiated THP-1 macrophages in each well were captured for further analysis using Image J software.

2.7. ImageJ analysis

All images were processed and analyzed with ImageJ 1.45 s (National Institutes of Health, USA), where the intensities of lipid droplets within the cells were quantified. First, the 8-bit red–green–blue ORO-stained images were converted into binary images consisting of only pixels that represent the lipid droplets. The acquired images were threshold for color saturation of the lipid droplets signal. Integrated density data from the analysis representing the amount of lipid droplets was obtained. Average values of the integrated density data obtained from three independent experiments were statistically analyzed by SPSS (version 25) using one-way analysis of variance (ANOVA) with Tukey's post hoc test to assess for significant differences between treatment groups. For all tests, $p < .05$ was considered significant.

2.8. Optimized cellular uptake of Dil-oxLDL

Uptake of DiI-oxLDL was analyzed using flow cytometric analysis. Native LDL was pre-labeled with Dil (0.15 mg/mL, final concentration;

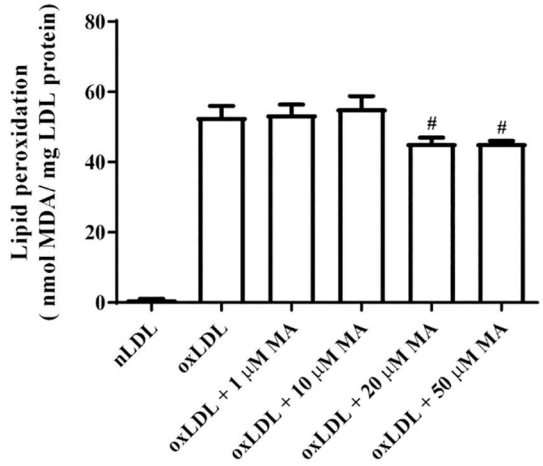

Fig. 4. MA inhibits $CuSO_4$-induced LDL oxidation. Oxidized LDL (oxLDL) is generated by incubating native LDL (nLDL) (2 mg/mL) with 50 μM $CuSO_4$ for 24 h at 37 ˚C. The potential of MA in inhibiting $CuSO_4$-induced LDL oxidation is determined by incubating nLDL with 50 μM $CuSO_4$ in the presence of various concentrations of MA (1, 10 and 20 μM). The extent of LDL oxidation was determined by measuring the amount of malondialdehyde (MDA) formed using Thiobarbituric acid reactive substances (TBARS) assay. The amount of MDA was determined by reading its absorbance at wavelength of 532 nm using Epoch" 2 microplate spectrophotometer. The results were expressed as nmol MDA/ mg LDL protein. Values represent means ± SD of three independent experiments performed in triplicates. Statistical significance was determined by One-way ANOVA followed by a Tukey's test where several experimental groups were compared to the control group. # represents $p < .05$ compared to oxLDL.

Sigma-Aldrich, US) and incubated overnight at 37 ˚C in before oxidation. Briefly, to prepare DiI-oxLDL, DiI-LDL (1.5 mg/mL) was incubated with $CuSO_4$ (50 μM, final concentration) at 37 ˚C for 24 h in dark. The PMA-differentiated THP-1 macrophages were serum starved for 24 h and treated with 50 μg/mL of Dil-oxLDL for 4 h. The cells were washed 3 times with ice-cold PBS containing 2 mg/mL BSA before trypsinization. The cells were harvested with trypsin (Invitrogen, US) and centrifuged at 4000 rpm for 5 min at 4 ˚C and washed twice with ice-cold PBS. Flow cytometric analysis was performed using Accuri C6 flow cytometer (BD Biosciences, USA). The fluorescence is detected on FL2 (585/40 nm) in log mode. A histogram with FL2 on x-axis and cell count on y-axis was set up to analyze gated populations of THP-1 macrophages. The cells were analyzed at slow flow rate (14 μL/min, 10 μm core). The mean fluorescence intensity (MFI) values were recorded.

2.9. Cholesterol efflux assay

PMA-differentiated THP-1 macrophages were first treated with or without 20 μM MA for 24 h at 37 ˚C, and then further incubate with 1 μg/mL 3-hexanoyl-NBD labeled cholesterol for 6 h. Following incubation, the cells were washed twice with PBS and incubated in RPMI-1640 for 4 h. The amount of cholesterol in the culture medium and cell lysates were determined by detecting the fluorescence intensity at wavelength range λ = 485 nm excitation/520 nm emission with BMG FLUOstar OPTIMA Microplate Reader. RIPA lysis buffer (Thermo scientific, USA) was used to lyse the cells in a 24-well culture plate, and the cells lysate was homogenized. A total volume of 450 μL was then aliquoted into three wells of a 96-well culture plate for the measurement of fluorescence intensity. The rate of cholesterol efflux was

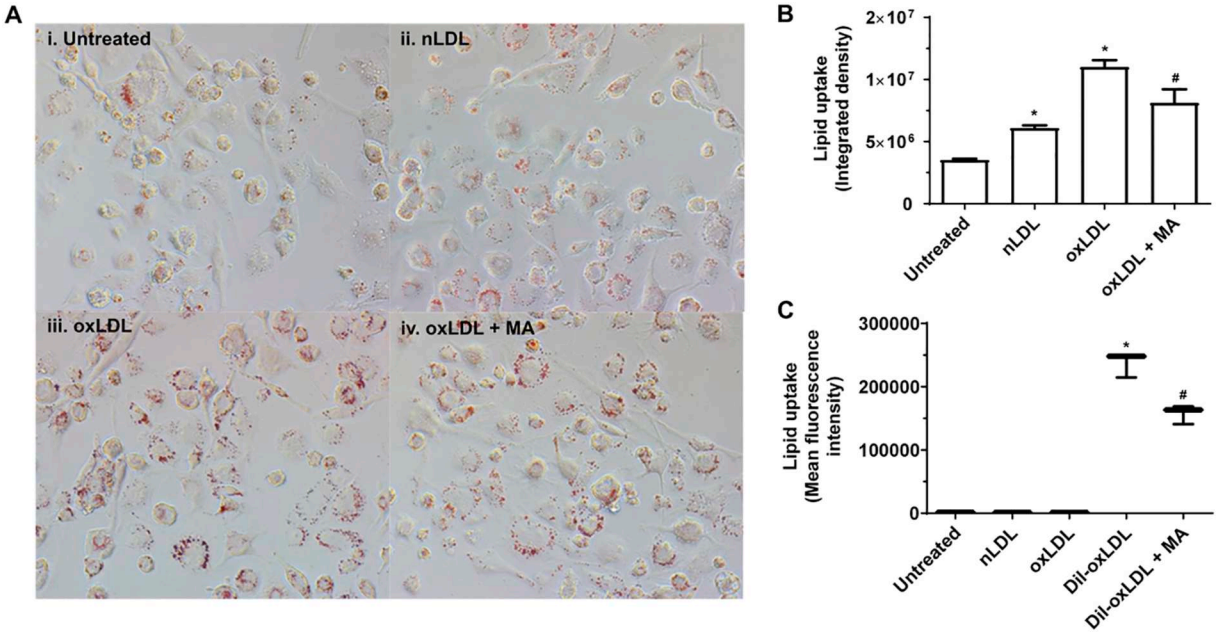

Fig. 5. MA suppresses macrophage foam cells formation. (**A**) ORO-stained images of THP-1 macrophages upon incubation with either native LDL (nLDL), $CuSO_4$-oxidized LDL (oxLDL) alone or in co-incubation with 20 μM MA. THP-1 macrophages were either (**i**) untreated, (**ii**) incubated with native LDL (nLDL), or (**iii**) incubated with $CuSO_4$-oxidized LDL (oxLDL) for 24 h. To determine the effect of MA on foam cell formation, THP-1 macrophages were either incubated with (**iv**) oxLDL in the presence of 20 μM MA. THP-1 macrophages were stained with ORO and foam cells formation was observed using Nikon eclipse Ti inverted microscopy at 200 x magnifications. (**B**) ORO-stained images were further analyzed by Image J software to determine the intensity of lipid droplets accumulated. (**C**) The effect of MA on oxLDL uptake was determined by flow cytometric analysis of macrophages internalizing Dil-labeled oxLDL. THP-1 macrophages in 24-well culture plate were either incubated with nLDL, oxLDL, Dil-oxLDL, or Dil-oxLDL in the presence of 20 μM MA for 4 h at 37 ˚C. Macrophages were then harvested, washed and analyzed by Accuri flow cytometry. Values represent means ± SD of three independent experiments performed in triplicates. Statistical significance was determined by One-way ANOVA followed by a Tukey's test where several experimental groups were compared to the control group. * represents $p < .05$ compared to untreated cells. # represents $p < .05$ compared to cells treated with oxLDL.

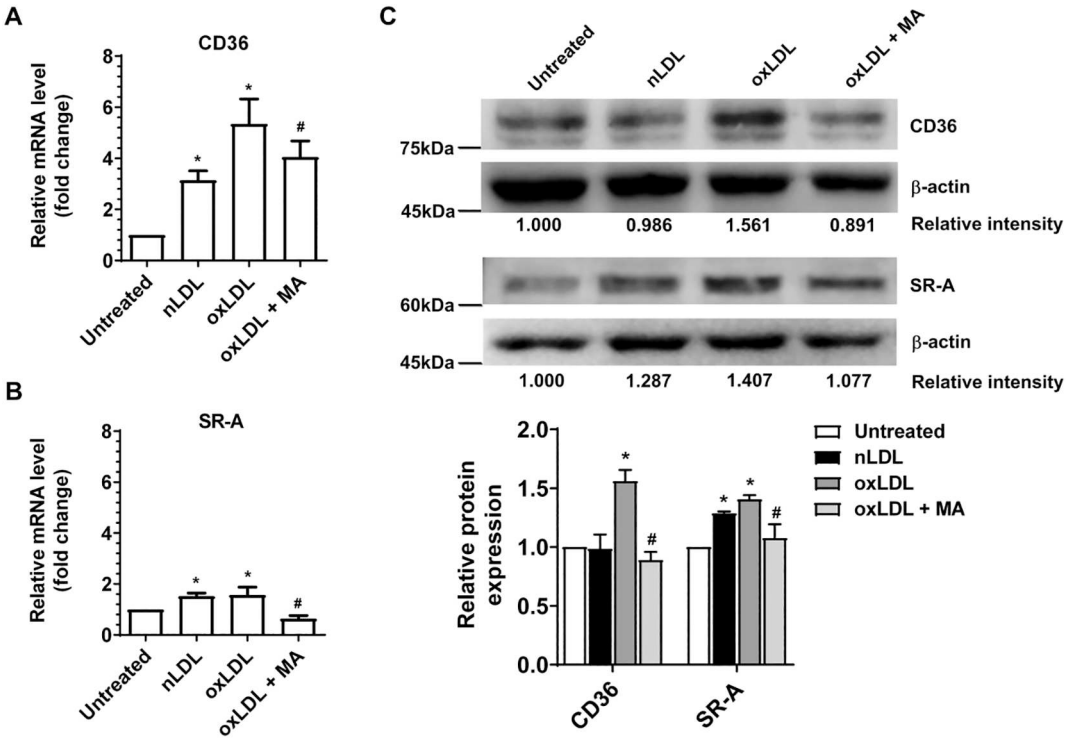

Fig. 6. MA reduces scavenger receptors CD36 and SR-A expression. (**A**) and (**B**) represent RT-qPCR analysis of CD36 and SR-A genes expression in THP-1 macrophages with different treatments. (**C**) represents Western blot analysis of CD36 and SR-A proteins expression in THP-1 macrophages with different treatments. Relative intensity, represented by the band intensity in Western blot, is summarized in the box plot. GAPDH and β-actin (45 kDa) served as the internal control. Values represent means ± SD of three independent experiments performed in triplicates. Statistical significance was determined by One-way ANOVA followed by a Tukey's test where several experimental groups were compared to the control group. * represent $p < .05$ compared to untreated cells. # represents $p < .05$ compared to oxLDL.

calculated by dividing the efflux value in medium with the total efflux value in medium and cells (treated and non-treated) and multiply by 100%. The result was expressed in percentage.

2.10. RT-PCR

Total RNA was isolated from HUVECs and PMA-differentiated THP-1 macrophages with a TRIzol reagent kit (Invitrogen, US). cDNA synthesis was performed on 300 ng of total RNA with qPCRBIO cDNA Synthesis Kit (PCR Biosystems, UK). The oligonucleotide primers for PCR were designed as follows: β-actin, forward, 5′-GCA TCC TGG GCT ACA CTG-3′, and reverse, 5′-GTG AGG AGG GGA GAT TCA G-3′; VCAM-1, forward, 5′-TCA GAT TGG AGA CTC AGT CAT GT-3′, and reverse, 5′-ACT CCT CAC CTT CCC GCT C-3′; MCP-1, forward, 5′-GCT CAG CCA GAT GCA ATC AA-3′, and reverse, 5′-GGT TGT GGA GTG AGT GTT CAA G-3′; SR-A, forward, 5′-GCA GTT CTC ATC CCT CTC AT-3′, and reverse, 5′-GGT ATT CTC TTG GAT TTT GCC-3′; CD36, forward, 5′-GAG AAC TGT TAT GGG GCT AT-3′, and reverse, 5′-TTC AAC TGG AGA GGC AAA GG-3′, ABCA1, forward, 5′-AACAGTTTGTGGCCCTTTTG-3′, and reverse, 5′-AGT TCC AGG CTG GGG TAC TT-3′; ABCG1, forward, 5′-CGG AGC CCA AGT CGG TGT-3′, and reverse, 5′-TTT CAG ATG TCC ATT CAG CAG GTC-3′.

2.11. Quantitative reverse transcription PCR (RT-qPCR)

RT-qPCR assays were performed to quantify the levels of mRNA in HUVECs (VCAM-1, MCP-1) and PMA-differentiated THP-1 macrophages (SR-A, CD36, ABCA1 and ABCG1). The RT-qPCR was performed using qPCRBIO SyGreen Blue Mix kit (PCR Biosystems, UK) according to manufacturer's instructions. Briefly, RT-qPCR assays in the Eppendorf Mastercycler® RealPlex2 (Eppendorf, Germany) used optimized 20 μL reaction mixtures containing 2× qPCRBIO SyGreen Blue Mix, 400 nM of forward and reverse primers, cDNA template and RNase-free water. The thermocycling protocols were described for each target gene. MCP-1, ABCA1 and ABCG1: Initial denaturation at 95 °C for 2 min, followed by 40 cycles of denaturation at 95 °C for 5 s and annealing at 60 °C for 30 s. VCAM-1: Initial denaturation at 95 °C for 2 min, followed by 40 cycles of denaturation at 95 °C for 15 s and annealing at 60 °C for 60 s. CD36 and SR-A: Initial denaturation at 95 °C for 2 min, followed by 40 cycles of denaturation at 95 °C for 5 s and annealing at 58.5 °C for 30 s. Each sample was measured in triplicate. Melting curve analyses were performed for the PCR products of all genes and GAPDH gene amplifications to evaluate primer specificity. The relative abundance of all gene expression were evaluated using the comparative Ct ($2^{-\Delta\Delta Ct}$) method and was normalized to GAPDH gene levels.

2.12. Western blot analysis

Cell extracts were prepared with M-PER Mammalian Protein Extraction Reagent (Thermo Scientific, USA). Protein concentrations were measured by a BCA Protein Assay Kit (Thermo Scientific, USA) using bovine serum albumin (BSA) as the standard. A total of 10 μg of protein samples from HUVECs (VCAM-1, MCP-1) and PMA-differentiated THP-1 macrophages (SR-A, CD36, ABCA1 and ABCG1) was subjected to 7.5% or 10% sodiumdodecyl sulfate-polyacrylamide gel electrophoresis (SDS-PAGE) using Bio-Rad compact power supply at 16 mA per gel and transferred to Bio-lott PVDF Transfer Membrane (Membrane Solution, USA) with 0.45 μm pore size. After regular blocking and washing, the membranes were incubated with primary antibodies [VCAM-1 (E1E8X) 1:1000, MCP-1 (sc-32,771) 1:1000 SR-A (MAB2708), 1:1000; CD36 (NB600-1423), 1:2000; ABCA1 (NB100-2068), 1:2000; ABCG1 (NB400-132), 1:500] overnight at 4 °C, followed by incubating with HRP-conjugated secondary antibodies [anti-rabbit

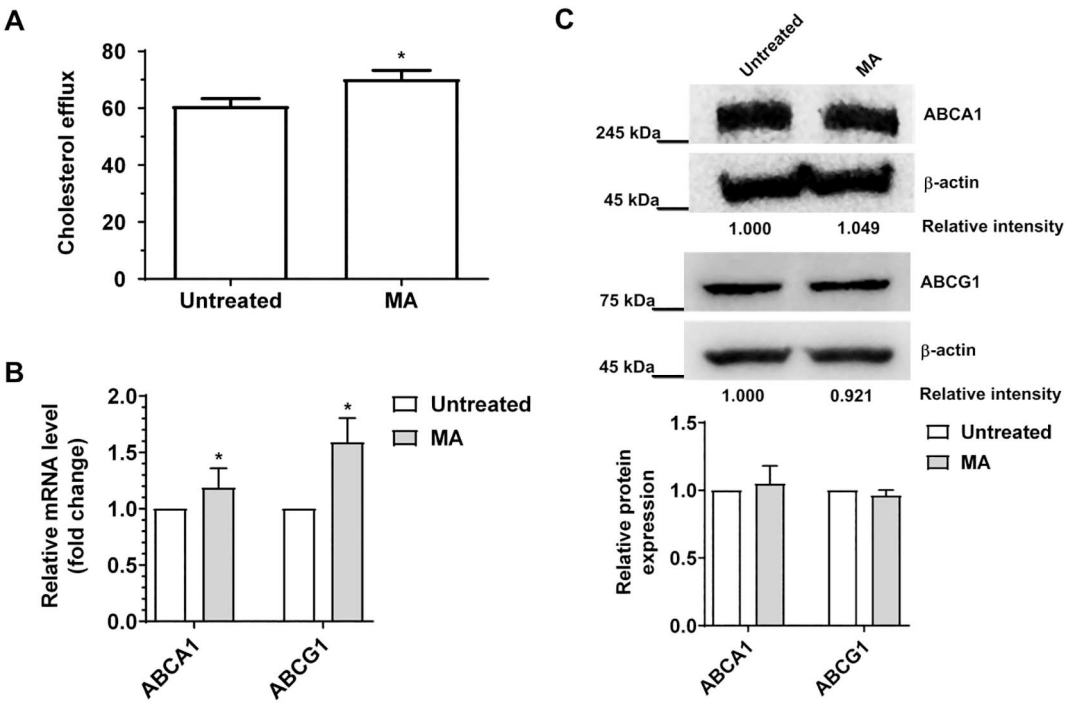

Fig. 7. MA enhanced cholesterol efflux from human THP-1 macrophages without affecting expression of efflux transporter proteins ABCA1 and ABCG1. (**A**) THP-1 macrophages were either untreated or pre-treated with 20 μM MA for 24 h at 37 °C, and then incubated with 1 μg/mL 3-hexanoyl-NBD labeled cholesterol for additional 6 h. After exposure to NBD-labeled cholesterol, the cells were washed twice with PBS and incubated in RPMI-1640 for 4 h. The fluorescence-labeled cholesterol of medium and cell lysates were detected at wavelength range λ = 485 nm excitation/520 nm emission by using BMG FLUOstar OPTIMA Microplate Reader. (**B**) represents RT-qPCR analysis of ABCA1 and ABCG1 genes expression in THP-1 macrophages with different treatments. (**C**) represents Western blot analysis of ABCA1 and ABCG1 proteins expression in THP-1 macrophages with different treatments. Relative intensity, represented by the band intensity in Western blot, is summarized in box plot. GAPDH and β-actin (45 kDa) served as the internal control. Values represent means ± SD of three independent experiments performed in triplicates. Statistical significance was determined by independent sample test. A value of $p < .05$ was considered statistically significant. * represents $p < .05$ statistical difference compared to untreated cells.

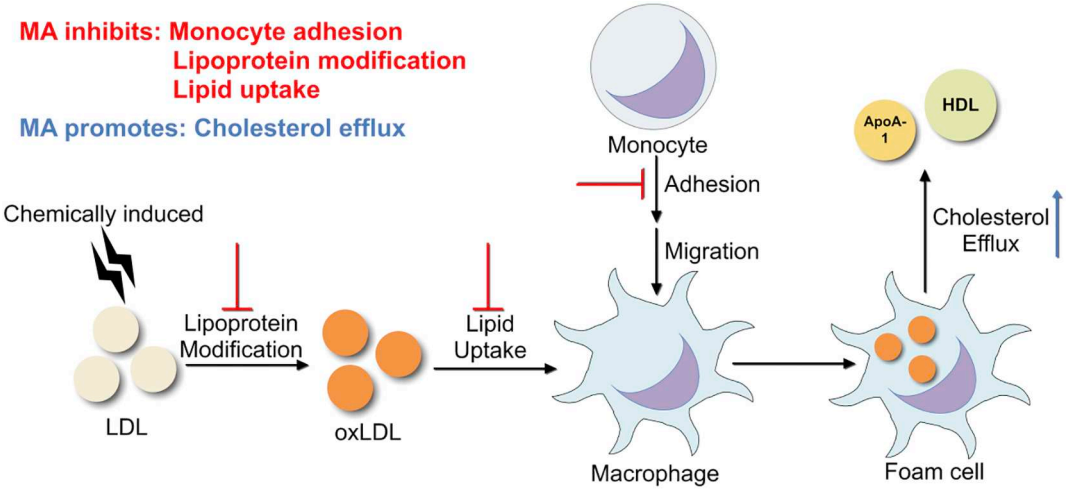

Fig. 8. Multiple targeting effects of MA on foam cell formation. MA exerts an atheroprotective effect by inhibiting LDL modification, reducing TNF-α-mediated monocyte adhesion to endothelial cells, LDL uptake as well as marginally promoting cholesterol efflux in macrophages. Red arrow indicates the suppression of foam cell formation process; blue arrow indicates induction of cholesterol efflux process. (For interpretation of the references to color in this figure legend, the reader is referred to the web version of this article.)

(7074), 1:3000; anti-mouse (NB7570), 1:5000] for 1 h at room temperature. β-actin (MAB8929; 1:50,000) was used for protein normalization. Signals were visualized using enhanced chemiluminescence detection reagents, Pierce ECL Western Blotting Substrate (Thermo Scientific, USA) and imaged using a Chemiluminescent gel doc (UVP GelDoc). Protein expression was then analyzed using ImageJ 1.45s (National Institutes of Health, USA). Three independent experiments were performed for each protein expression analysis. The protein quantification of the Western blot results were normalized to β-actin and then compared to the control group.

2.13. Statistical analysis

All experimental data were expressed as mean ± SD. All

experiments were performed independently with three replicates each. Statistical analysis was performed by SPSS (version 25) using one-way analysis of variance (ANOVA) to assess significant differences between treatment groups. Images from ORO staining were quantified using the ImageJ 1.45 s (National Institute of Health, USA). For all tests, $p < .05$ is considered significant.

3. Results

3.1. Cytotoxic effects of MA on HUVECs, THP-1 monocytes and PMA-differentiated THP-1 macrophages

In order to determine whether MA (Fig. 1A) affects the growth of cell lines used in this experiment, its cytotoxic effects was measured using Resazurin assay (Fig. 1B, C, D). Dimethyl sulfoxide (DMSO) was used to dissolve MA and it was included as a vehicle control (0.5%) in the untreated samples. MA at 10 μM concentration showed significant cytotoxic effects against HUVECs and THP-1 monocytes. However, MA only showed cytotoxicity effect on PMA-differentiated THP-1 macrophages at 50 μM onwards. In this experiment, sub-cytotoxic concentrations of MA were selected for subsequent cell treatments. MA at 5 μM concentration was used for HUVECs and THP-1 monocytes while 20 μM MA was used for PMA-differentiated THP-1 macrophages for the following experiments.

3.2. MA reduces TNF-α-induced monocyte adhesion to endothelial cells, VCAM-1 and MCP-1 protein expression

In order to determine how MA affects monocyte recruitment to endothelial cells, its effect on several monocytes adhesion models were determined (Fig. 2A and Supplementary Fig. S1). Briefly, four separate models were investigated where MA was either co-incubated with TNF-α-induced HUVECs or Calcein-labeled THP-1 monocytes at different time points to analyze its effect on monocyte adhesion. It was shown that incubation of HUVECs with TNF-α for 24 h significantly induced monocytes adhesion (Fig. 2A; Supplementary Fig. S1A and S1B), but the effects were not observed in TNF-α-induced THP-1 monocytes (Supplementary Fig. S1C and S1D).

Results have shown that MA (at sub-cytotoxic concentrations 5 μM) significantly suppresses TNF-α-induced monocytes adhesion. It should however be noted that incubation with MA alone (5 μM) also resulted in significantly lower monocytes adhesion, indicating that MA could block monocytes adhesion in a TNF-α-dependent and independent manner (Fig. 2A). It was further demonstrated in a different model (Supplementary Fig. S1B) where co-incubation of MA and Calcein-labeled monocytes for 1 h on TNF-α-induced HUVECs could block monocytes adhesion in a TNF-α-independent manner. We further investigate the effect of MA on trans-endothelial migration using a Transwell co-culture model comprising of TNF-α-induced HUVECs and Calcein-labeled THP-1 monocytes. As shown in Fig. 2B, addition of recombinant human TNF-α enhanced trans-endothelial migration. However, incubation with MA alone at 5 μM enhances transmigration.

Considering that MA inhibits THP-1 monocytes adhesion on HUVECs, we postulated that MA might down-regulate both the expression of functional adhesion molecules expression in HUVECs. As shown in Fig. 3A and B, a significant down-regulation of VCAM-1 and MCP-1 ($p = .000$) gene expression was observed in both HUVECs treated with MA (5 and 10 μM) and TNF-α when compared to TNF-α-induced HUVECs. As expected, TNF-α increases the gene expressions of VCAM-1 and MCP-1. Similarly, results obtained from Western blot, a significant up-regulation in both the expression of VCAM-1 ($p = .000$) and MCP-1 ($p = .000$) were observed in TNF-α-induced HUVECs compared to the untreated HUVECs (Fig. 3C) while incubation with MA (5 and 10 μM) and TNF-α demonstrated a significant reduction of VCAM-1 and MCP-1 protein expression ($p = .000$) compared to TNF-α-induced HUVECs. Addition of MA alone did not affect VCAM-1and MCP-1 expression.

3.3. MA inhibits foam cell formation

Considering MA suppresses monocyte recruitment to the endothelial layer, we further examined its protective effects against lipids peroxidation and macrophage foam cells formation. As shown in Fig. 4, $CuSO_4$ significantly enhanced LDL oxidation when compared to native LDL alone. Addition of MA at 20 μM and 50 μM shows a significant reduction of lipid peroxidation when compared to control group, indicating that MA has potential antioxidant effect on CuSO4-induced LDL oxidization. Further study was performed to examine whether MA could inhibit macrophages foam cells formation through analyzing its effects on intracellular lipids accumulation in THP-1 macrophages using ORO staining. MA was shown to significantly reduce intracellular lipid droplet accumulation in THP-1 macrophages when incubated with oxLDL and 20 μM MA ($p = .000$) (Fig. 5A and B). Flow cytometric analysis was used to determine the uptake of oxLDL within macrophages. As shown in Fig. 5C, THP-1 macrophages was shown to exhibit enhanced uptake of Dil-labeled oxLDL ($p = .000$). A significant reduction in the uptake of oxLDL was shown when THP-1 macrophages were incubated with oxLDL and MA for 24 h.

3.4. MA down-regulates scavenger receptors SR-A and CD36 expression

It is hypothesized that MA may have down-regulate the expression of macrophage scavenger receptor A (SR-A) and class B scavenger receptor CD36 (CD36) based on the ORO staining and flow cytometric analysis as both of these receptor contribute to foam cell formation and atherogenesis via uptake of modified lipoproteins. As shown in Fig. 6A and B, a significant down-regulation of SR-A and CD36 ($p = .000$) gene expression was observed in both THP-1 macrophages treated with oxLDL and MA when compared to THP-1 macrophages incubated only with oxidized LDL. Similarly, Western blot analysis (Fig. 6C) showed that CD36 and SR-A protein expressions were significantly decreased when compared to THP-1 macrophage treated with oxidized LDL. It is suggested that MA works by inhibiting both during $CuSO_4$-induced LDL oxidation as well as after LDL oxidation take place, thereby resulting in the inhibition of foam cells formation.

3.5. MA enhances cholesterol efflux from THP-1 macrophages

Meanwhile, addition of MA was shown to significantly increase the cholesterol efflux capacity as compared to untreated cells (Fig. 7A). Cholesterol transporter ABCA1 and ABCG1 gene and protein expression in THP-1 macrophages was further analyzed due to its important role in cholesterol uptake from macrophage and phospholipids homeostasis which helps in decreasing the formation of foam cells. As shown in Fig. 7B, a significant up-regulation of ABCA1 and ABCG1 gene expression was observed when THP-1 macrophages pre-treated with MA for 24 h. Contrary to the RT-qPCR analysis, addition of MA on THP-1 macrophages does not have effect on ABCA1 and ABCG1 genes and proteins expression (Fig. 7C).

4. Discussion

Inflammatory process plays a key role in various stages of plaque development. This includes the activation of endothelial cells leading to monocyte adhesion. Endothelial cell activation can be initiated by inflammatory stimuli (LPS, TNF-α, IL-1β) during endothelial dysfunction, which increases the expression of monocyte adhesion molecules including *E*-selectin, P-selectin, VCAM-1 and ICAM-1 and promotes monocytes recruitment to the intima layer. Monocytes have been reported to adhere to endothelial cell monolayers in vitro [5,18–21]. In this study, TNF-α was used to stimulate the monocyte-endothelial adhesion and migration in vitro. Indeed, TNF-α enhanced endothelial

adhesion and migration of THP-1 monocytes. MA has been widely reported as a natural compound with anti-oxidant and anti-inflammatory as well as cardioprotective effects [22–24]. Addition of MA at 5 μM and 10 μM alone and combination of TNF-α significantly suppresses THP-1 monocytes adhesion to endothelial cells, indicating MA could block monocytes adhesion in a TNF-α-dependent and independent manner.

There are accumulating evidences suggesting that TNF-α induces vascular inflammation, vascular oxidative stress, monocyte adhesion to endothelial cells and atherogenic response and take part in the regulation of thrombosis and coagulation through multiple signaling pathways including NF-κB, activator protein 1, p38, Sp1, JNK and STAT3 [1]. Various natural compounds are known to delay or prevent the development of vascular disorders. For example, apigenin was found blocking monocyte adhesion to HUVECs by suppressing TNF-α-induced up-regulation of VCAM-1, ICAM-1, and E-selectin mRNA expression [25]. Studies also demonstrate that epigallocatechin gallate decreased TNF-α-induced fractalkine expression by suppressing NF-κB and inhibited TNF-α-induced MCP-1 production as well as the activation of AP-1 in vascular endothelial cells via heme oxygenase-1-dependent pathway [26–28]. Previous study also reported that gingerenone A attenuates TNF-α and LPS-induced monocyte adhesion and the expression of adhesion factors VCAM-1 and CCL2 in endothelial cells via the suppression of NF-κB signaling [29]. Similar study confirmed the suppressive effects of MA on LPS-induced TNF production and the expression of inflammatory response associated genes in RAW 264.7 cells along with the suppressive effect of MA acid on LPS-induced NF-κB activation as well as the phosphorylation of IκB-α [23]. In the present study, treatment with MA inhibited significantly VCAM-1 and MCP-1 expressions, indicating that MA has similar anti-inflammatory and vasoprotective properties.

Following monocyte recruitment to the subendothelial layer, monocytes can transform into macrophages and take up modified lipoprotein particles such as oxLDL through scavenger receptors within the arterial intima, which lead to the formation of foam cells. In this study, MA suppresses foam cells formation as indicated in the reduced intracellular lipids accumulation from ORO staining and Dil-LDL uptake analysis. It was reported that MA decreased the serum MDA levels by inhibiting lipid peroxides production in Wistar rat [30]. In addition, MA demonstrated copper chelating effect and inhibited $CuSO_4$-induced LDL oxidation [31,32]. The antioxidant effect of MA was also demonstrated in this study where addition of MA attenuates $CuSO_4$-induced lipid peroxidation in THP-1 macrophages. These observations suggest that MA may affect macrophage foam cells formation by suppressing LDL oxidation and their subsequent accumulation in macrophages. Recent study also reported that ethanol extract from Dan-Lou prescription and simvastatin treatment decrease oxLDL-induced lipid accumulation and inhibited the binding and internalization of Dil-ox-LDL in RAW 264.7 cells in the process of Dil-ox-LDL uptake via the TLR4/NF-κB and PPARγ Signaling Pathways [33].

Apart from targeting LDL oxidation, MA was also investigated for their role in regulating oxLDL receptors responsible for lipids uptake. It is known that scavenger receptors SR-A and CD36 contribute in foam cell formation during atherogenesis and in the regulation of inflammatory signaling pathways. Studies also confirmed that CD36-dependent signaling pathway initiated by oxLDL [34] together with up-regulated expression of SR-A in human monocyte or macrophages leads to increased lipid uptake and foam cell formation [35]. Meanwhile, a study found that combined loss of SR-A and CD36 had a significant suppressive effect on inflammatory gene expression and advanced lesional macrophage apoptosis and plaque necrosis [36]. Our results showed that MA significantly suppressed both gene and protein expression of SR-A and CD36 in THP-1 macrophages, which may contribute to inhibition of foam cell formation.

Meanwhile, cholesterol efflux is an atheroprotective process that counteracts macrophages foam cell formation. Cellular cholesterol efflux is mediated by ATP-binding cassette transporters such as ABCA1 and ABCG1. Previous studies also demonstrated that up-regulation of ABC transporters genes and protein expression by Tanshinone IIA and salidroside promoted cholesterol efflux from macrophages, thereby reducing cholesterol accumulation [12,37]. Therefore, we hypothesized that MA might regulate the cholesterol efflux pathway from THP-1 macrophages. Our study indicates that MA significantly up-regulated ABCA1 and ABCG1 genes expression in THP-1 macrophages but no effects on ABCA1 and ABCG1 proteins expression (Fig. 8).

MA (2-α, 3-β-dihydroxyolean-12-en-28-oic acid) has been known to possess a wide-range of health effects, including anti-oxidant, anti-inflammatory, and anti-tumor properties, in experimental models [38,39]. In support of its anti-inflammatory and cardioprotective properties, MA was shown to inhibit TNF-α-induced adhesion molecule expression through the inhibitory action on NF-κB subunit p65 translocation to the nucleus, which was correlated with a lower phosphorylation of IκBα [13,40]. This study reports that MA is capable in blocking TNF-α and its downstream pro-atherosclerotic effects on endothelial cells, inhibits LDL oxidation and foam cells formation through suppressing scavenger receptors expression while enhancing cholesterol efflux.

In summary, MA may exerts multiple effects in suppressing foam cell formation process and may have potential for therapeutic use in preventing atherosclerotic lesions and other inflammatory diseases. In view of the research results, the specific mechanism of MA in foam cell formation process remains to be determined.

Supplementary data to this article can be found online at https://doi.org/10.1016/j.vph.2020.106675.

Declaration of Competing Interest

The authors declare no conflict of interest.

Acknowledgments

The authors would like to thank Ministry of Education Malaysia (MOE) Fundamental Research Grant Scheme for funding support (Fundamental Research Grant Scheme FRGS/1/2015/SKK08/TAYLOR/03/1).

References

[1] H. Zhang, C. Zhang, Vasoprotection by dietary supplements and exercise: role of TNFα signaling, Exp. Diabetes Res. 2012 (2012) 972679, https://doi.org/10.1155/2012/972679.
[2] S.J. O'Carroll, D.T. Kho, R. Wiltshire, V. Nelson, O. Rotimi, R. Johnson, C.E. Angel, E.S. Graham, Pro-inflammatory TNFα and IL-1β differentially regulate the inflammatory phenotype of brain microvascular endothelial cells, J. Neuroinflammation 12 (2015) 131, https://doi.org/10.1186/s12974-015-0346-0.
[3] E. Galkina, K. Ley, Immune and inflammatory mechanisms of atherosclerosis, Annu. Rev. Immunol. 27 (2009) 165–197, https://doi.org/10.1146/annurev.immunol.021908.132620.
[4] J. Mai, A. Virtue, J. Shen, H. Wang, X.-F. Yang, An evolving new paradigm: endothelial cells–conditional innate immune cells, J. Hematol. Oncol. 6 (2013) 61, https://doi.org/10.1186/1756-8722-6-61.
[5] M. Takahashi, U. Ikeda, J.-I. Masuyama, S.-I. Kitagawa, T. Kasahara, M. Shimpo, S. Kano, K. Shimada, Monocyte-endothelial cell interaction induces expression of adhesion molecules on human umbilical cord endothelial cells, Cardiovasc. Res. 32 (1996) 422–429, https://doi.org/10.1016/0008-6363(96)00085-5.
[6] J. Varga, Chapter 83 - etiology and pathogenesis of scleroderma, in: G.S. Firestein, R.C. Budd, S.E. Gabriel, I.B. McInnes, J.R. O'Dell (Eds.), Kelley and Firestein's Textbook of Rheumatology (Tenth Edition), Elsevier, 2017, , https://doi.org/10.1016/B978-0-323-31696-5.00083-8pp (1400–1423.e1403).
[7] J.M. Cook-Mills, M.E. Marchese, H. Abdala-Valencia, Vascular cell adhesion molecule-1 expression and signaling during disease: regulation by reactive oxygen species and antioxidants, Antioxid. Redox Signal. 2011 (1607-1638) 15, https://doi.org/10.1089/ars.2010.3522.
[8] X.-H. Yu, Y.-C. Fu, D.-W. Zhang, K. Yin, C.-K. Tang, Foam cells in atherosclerosis, Clin. Chim. Acta 424 (2013) 245–252, https://doi.org/10.1016/j.cca.2013.06.006.
[9] S. Samson, L. Mundkur, V.V. Kakkar, Immune response to lipoproteins in atherosclerosis, Cholesterol 2012 (2012) 12, https://doi.org/10.1155/2012/571846.
[10] K. Mokhtari, E.E. Rufino-Palomares, A. Perez-Jimenez, F.J. Reyes-Zurita, C. Figuera, L. García-Salguero, P.P. Medina, J. Peragón, J.A. Lupiáñez, et al., Maslinic Acid, a triterpene from olive, affects the antioxidant and mitochondrial status of B16F10

melanoma cells grown under stressful conditions, Evid. Based Complement. Alternat. Med. 2015 (2015) 11, https://doi.org/10.1155/2015/272457.
[11] F.J. Reyes-Zurita, E.E. Rufino-Palomares, L. García-Salguero, J. Peragón, P.P. Medina, A. Parra, M. Cascante, J.A. Lupiáñez, Maslinic acid, a natural triterpene, induces a death receptor-mediated apoptotic mechanism in Caco-2 p53-deficient colon adenocarcinoma cells, PLoS One 11 (2016) e0146178, , https://doi.org/10.1371/journal.pone.0146178.
[12] Z. Liu, J. Wang, E. Huang, S. Gao, H. Li, J. Lu, K. Tian, P.J. Little, X. Shen, S. Xu, et al., Tanshinone IIA suppresses cholesterol accumulation in human macrophages: role of heme oxygenase-1, J. Lipid Res. 55 (2014) 201–213, https://doi.org/10.1194/jlr.M040394.
[13] G. Lozano-Mena, M. Sánchez-González, M.E. Juan, J.M. Planas, Maslinic acid, a natural phytoalexin-type triterpene from olives-a promising nutraceutical? Molecules 19 (2014) 11538–11559, https://doi.org/10.3390/molecules190811538.
[14] C. Sánchez-Quesada, A. López-Biedma, J.J. Gaforio, Maslinic acid enhances signals for the recruitment of macrophages and their differentiation to m1 state, Evid. Based Complement. Alternat. Med. 2015 (2015) 654721, https://doi.org/10.1155/2015/654721.
[15] C. Moneriz, P. Marín-García, J.M. Bautista, A. Diez, A. Puyet, Parasitostatic effect of maslinic acid. II. Survival increase and immune protection in lethal Plasmodium yoelii-infected mice, Malar. J. 10 (2011) 103, https://doi.org/10.1186/1475-2875-10-103.
[16] A. Hussain Shaik, S.N. Rasool, M.A. Kareem, G.S. Krushna, P.M. Akhtar, K.L. Devi, Maslinic acid protects against isoproterenol-induced cardiotoxicity in albino Wistar rats, J. Med. Food 15 (2012) 741–746, https://doi.org/10.1089/jmf.2012.2191.
[17] J. Liu, H. Sun, X. Wang, D. Mu, H. Liao, L. Zhang, Effects of oleanolic acid and maslinic acid on hyperlipidemia, Drug Dev. Res. 68 (2007) 261–266, https://doi.org/10.1002/ddr.20187.
[18] D.J. Lowe, K. Raj, Quantitation of endothelial cell adhesiveness in vitro, J. Vis. Exp. (**2015**), https://doi.org/10.3791/52924 (e52924-e52924).
[19] S.J. Lee, S.E. Baek, M.A. Jang, C.D. Kim, SIRT1 inhibits monocyte adhesion to the vascular endothelium by suppressing Mac-1 expression on monocytes, Exp. Mol. Med. 51 (2019) 47, https://doi.org/10.1038/s12276-019-0239-x.
[20] H. Yamada, M. Yoshida, Y. Nakano, T. Suganami, N. Satoh, T. Mita, K. Azuma, M. Itoh, Y. Yamamoto, Y. Kamei, et al., In vivo and in vitro inhibition of monocyte adhesion to endothelial cells and endothelial adhesion molecules by eicosapentaenoic acid, Arterioscler. Thromb. Vasc. Biol. 28 (2008) 2173–2179, https://doi.org/10.1161/ATVBAHA.108.171736.
[21] J. Meerschaert, M.B. Furie, The adhesion molecules used by monocytes for migration across endothelium include CD11a/CD18, CD11b/CD18, and VLA-4 on monocytes and ICAM-1, VCAM-1, and other ligands on endothelium, J. Immunol. 154 (1995) 4099–4112.
[22] S. Acín, M.A. Navarro, J.S. Perona, J.M. Arbonés-Mainar, J.C. Surra, M.A. Guzmán, R. Carnicer, C. Arnal, I. Orman, J.C. Segovia, et al., Olive oil preparation determines the atherosclerotic protection in apolipoprotein E knockout mice, J. Nutr. Biochem. 18 (2007) 418–424, https://doi.org/10.1016/j.jnutbio.2006.08.005.
[23] S. Fukumitsu, M.O. Villareal, T. Fujitsuka, K. Aida, H. Isoda, Anti-inflammatory and anti-arthritic effects of pentacyclic triterpenoids maslinic acid through NF-κB inactivation, Mol. Nutr. Food Res. 60 (2016) 399–409, https://doi.org/10.1002/mnfr.201500465.
[24] L. Huang, T. Guan, Y. Qian, M. Huang, X. Tang, Y. Li, H. Sun, Anti-inflammatory effects of maslinic acid, a natural triterpene, in cultured cortical astrocytes via suppression of nuclear factor-kappa B, Eur. J. Pharmacol. 672 (2011) 169–174, https://doi.org/10.1016/j.ejphar.2011.09.175.
[25] J.-H. Lee, H.Y. Zhou, S.Y. Cho, Y.S. Kim, Y.S. Lee, C.S. Jeong, Anti-inflammatory mechanisms of apigenin: inhibition of cyclooxygenase-2 expression, adhesion of monocytes to human umbilical vein endothelial cells, and expression of cellular adhesion molecules, Arch. Pharm. Res. 30 (2007) 1318–1327, https://doi.org/10.1007/BF02980273.
[26] H.Y. Ahn, Y. Xu, S.T. Davidge, Epigallocatechin-3-O-gallate inhibits TNFα-induced monocyte chemotactic protein-1 production from vascular endothelial cells, Life Sci. 82 (2008) 964–968, https://doi.org/10.1016/j.lfs.2008.02.018.
[27] A.S. Lee, Y.J. Jung, D.H. Kim, T.H. Lee, K.P. Kang, S. Lee, N.H. Lee, M.J. Sung, D.Y. Kwon, S.K. Park, et al., Epigallocatechin-3-O-gallate decreases tumor necrosis factor-alpha-induced fractalkine expression in endothelial cells by suppressing NF-kappaB, Cell. Physiol. Biochem. 24 (2009) 503–510, https://doi.org/10.1159/000257494.
[28] Y. Zheng, M. Toborek, B. Hennig, Epigallocatechin gallate-mediated protection against tumor necrosis factor-α-induced monocyte chemoattractant protein-1 expression is heme oxygenase-1 dependent, Metab. Clin. Exp. 59 (2010) 1528–1535, https://doi.org/10.1016/j.metabol.2010.01.018.
[29] H.J. Kim, J.E. Son, J.H. Kim, C.C. Lee, H. Yang, S.S. Yaghmoor, Y. Ahmed, J.M. Yousef, K.O. Abualnaja, A.L. Al-Malki, et al., Gingerenone a attenuates monocyte-endothelial adhesion via suppression of I kappa B kinase phosphorylation, J. Cell. Biochem. 119 (2018) 260–268, https://doi.org/10.1002/jcb.26138.
[30] M.P. Montilla, A. Agil, M.C. Navarro, M.I. Jiménez, A. García-Granados, A. Parra, M.M. Cabo, Antioxidant activity of maslinic acid, a triterpene derivative obtained from Olea europaea, Planta Med. 69 (2003) 472–474, https://doi.org/10.1055/s-2003-39698.
[31] Y. Allouche, G. Beltrán, J.J. Gaforio, M. Uceda, M.D. Mesa, Antioxidant and antiatherogenic activities of pentacyclic triterpenic diols and acids, Food Chem. Toxicol. 48 (2010) 2885–2890, https://doi.org/10.1016/j.fct.2010.07.022.
[32] R. Wang, W. Wei, L. Wang, R. Liu, D. Yi, L. Du, Constituents of the flowers of Punica granatum, Fitoterapia 77 (2006) 534–537, https://doi.org/10.1016/j.fitote.2006.06.011.
[33] L.-N. Gao, X. Zhou, Y.-R. Lu, K. Li, S. Gao, C.-Q. Yu, Y.-L. Cui, Dan-Lou prescription inhibits foam cell formation induced by ox-LDL via the TLR4/NF-κB and PPARγ signaling pathways, Front. Physiol. 9 (2018) 590.
[34] S.O. Rahaman, D.J. Lennon, M. Febbraio, E.A. Podrez, S.L. Hazen, Roy L. Silverstein, A CD36-dependent signaling cascade is necessary for macrophage foam cell formation, Cell Metab. 4 (2006) 211–221, https://doi.org/10.1016/j.cmet.2006.06.007.
[35] J. Li, Q. Fu, H. Cui, B. Qu, W. Pan, N. Shen, C. Bao, Interferon-α priming promotes lipid uptake and macrophage-derived foam cell formation: a novel link between interferon-α and atherosclerosis in lupus, Arthritis Rheum. 63 (2011) 492–502, https://doi.org/10.1002/art.30165.
[36] J.J. Manning-Tobin, K.J. Moore, T.A. Seimon, S.A. Bell, M. Sharuk, J.I. Alvarez-Leite, M.P.J. de Winther, I. Tabas, M.W. Freeman, Loss of SR-A and CD36 activity reduces atherosclerotic lesion complexity without abrogating foam cell formation in hyperlipidemic mice, Arterioscler. Thromb. Vasc. Biol. 29 (2009) 19–26, https://doi.org/10.1161/ATVBAHA.108.176644.
[37] J. Ni, Y. Li, W. Li, R. Guo, Salidroside protects against foam cell formation and apoptosis, possibly via the MAPK and AKT signaling pathways, Lipids Health Dis. 16 (2017) 198, https://doi.org/10.1186/s12944-017-0582-7.
[38] B.N. Mkhwanazi, M.R. Serumula, R.B. Myburg, F.R. Van Heerden, C.T. Musabayane, Antioxidant effects of maslinic acid in livers, hearts and kidneys of streptozotocin-induced diabetic rats: effects on kidney function, Ren. Fail. 36 (2014) 419–431, https://doi.org/10.3109/0886022X.2013.867799.
[39] C. Li, Z. Yang, C. Zhai, W. Qiu, D. Li, Z. Yi, L. Wang, J. Tang, M. Qian, J. Luo, et al., Maslinic acid potentiates the anti-tumor activity of tumor necrosis factor α by inhibiting NF-κB signaling pathway, Mol. Cancer 9 (2010) 73, https://doi.org/10.1186/1476-4598-9-73.
[40] E. Ampofo, J.J. Berg, M.D. Menger, M.W. Laschke, Maslinic acid alleviates ischemia/reperfusion-induced inflammation by downregulation of NFκB-mediated adhesion molecule expression, Sci. Rep. 9 (2019) 6119, https://doi.org/10.1038/s41598-019-42465-7.